

# Statistical Multifragmentation in Thermodynamical Limit: An Exact Solution for Phase Transitions

K.A. Bugaev<sup>1,2</sup>, M.I. Gorenstein<sup>1,2</sup>, I.N. Mishustin<sup>1,3,4</sup> and  
W. Greiner<sup>1</sup>

<sup>1</sup> Institut für Theoretische Physik, Universität Frankfurt, Germany

<sup>2</sup> Bogolyubov Institute for Theoretical Physics, Kyiv, Ukraine

<sup>3</sup> Kurchatov Institute, Russian Research Center, Moscow, Russia

<sup>4</sup> Niels Bohr Institute, University of Copenhagen, Denmark

## Abstract

An exact analytical solution of the statistical multifragmentation model is found in thermodynamic limit. Excluded volume effects are taken into account in the thermodynamically self-consistent way. The model exhibits a 1-st order phase transition of the liquid-gas type. An extension of the model including the Fisher's term is also studied. The possibility of the second order phase transition at or above the critical point is discussed. The mixed phase region of the phase diagram, where the gas of nuclear fragments coexists with the infinite liquid condensate, is unambiguously identified. The peculiar thermodynamic properties of the model near the boundary between the mixed phase and the pure gaseous phase are studied. The results for the caloric curve and specific heat are presented and a physical picture of the nuclear liquid-gas phase transition is clarified.

**Key words:** Nuclear matter, 1-st order liquid-gas phase transition,  
mixed phase thermodynamics

PACS: 21.65.+f, 24.10. Pa, 25.70. Pq

Nuclear multifragmentation is one of the most interesting and widely discussed phenomena in intermediate energy nuclear reactions. The statistical multifragmentation model (SMM) (see [1, 2] and references therein) was recently applied to study the liquid-gas phase transition in nuclear matter [3, 4, 5, 6]. Numerical calculations within the canonical ensemble exhibited many intriguing peculiarities of the finite multifragment systems. However, the investigation of the system's behavior in the thermodynamic limit was still missing. Therefore, there was no rigorous proof of the phase transition existence, and the phase diagram structure of the SMM remained unclear. Previous numerical studies for the finite nuclear systems (the canonical and microcanonical ensembles) led to unjustified (and sometimes wrong) statements concerning the nuclear liquid-gas phase transition in the thermodynamic limit. In our recent paper [7] an exact analytical solution of the SMM was found within the grand canonical ensemble which naturally allowed to study the thermodynamic limit. The self-consistent treatment of the excluded volume effects was an important part of this study. In this letter we investigate the peculiar thermodynamic properties near the boundary between the mixed phase and the pure gaseous phase. New results for the caloric curve and the specific heat are presented and a physical picture of the nuclear liquid-gas phase transition in SMM is clarified. This physical picture differs from the one advocated in the previous numerical studies.

In the SMM the states of the system are specified by the multiplicity sets  $\{n_k\}$  ( $n_k = 0, 1, 2, \dots$ ) of  $k$ -nucleon fragments. The partition function of a single fragment with  $k$  nucleons is [1]:  $\omega_k = V (mTk/2\pi)^{3/2} z_k$ , where  $k = 1, 2, \dots, A$  ( $A$  is the total number of nucleons in the system).  $V$  and  $T$  are, respectively, the volume and the temperature of the system,  $m$  is the nucleon mass. The first two factors in  $\omega_k$  originate from the non-relativistic thermal motion and the last factor,  $z_k$ , represents the intrinsic partition function of the  $k$ -fragment. For  $k = 1$  (nucleon) we take  $z_1 = 4$  (4 internal spin-isospin states) and for fragments with  $k > 1$  we use the expression motivated by the liquid drop model (see details in Ref. [1]):  $z_k = \exp(-f_k/T)$ , with the fragment free energy

$$f_k = -[W_o + T^2/\epsilon_o]k + \sigma(T) k^{2/3} + \tau T \ln k . \quad (1)$$

Here  $W_o = 16$  MeV is the bulk binding energy per nucleon,  $T^2/\epsilon_o$  is the contribution of the excited states taken in the Fermi-gas approximation ( $\epsilon_o = 16$  MeV) and  $\sigma(T)$  is the temperature dependent surface tension which is parameterized in the following form:

$$\sigma(T) = \sigma_o[(T_c^2 - T^2)/(T_c^2 + T^2)]^{5/4}, \quad (2)$$

with  $\sigma_o = 18$  MeV and  $T_c = 18$  MeV ( $\sigma = 0$  at  $T \geq T_c$ ). The last Fisher's term in Eq. (1) with dimensionless parameter  $\tau$  is introduced for generality. The canonical partition function (CPF) of the ensemble of nuclear fragments has the following form:

$$Z_A^{id}(V, T) = \sum_{\{n_k\}} \prod_{k=1}^A \frac{\omega_k^{n_k}}{n_k!} \delta(A - \sum_k kn_k) . \quad (3)$$

The model defined by Eqs.(1,3) with  $\tau = 0$  was studied numerically in Refs. [3, 4, 5, 6]. This is a simplified version of the SMM since the symmetry-energy and Coulomb contributions are neglected. However, its investigation appears to be very important for understanding the physics of multifragmentation.

In Eq. (3) the nuclear fragments are treated as point-like objects. However, these fragments have non-zero proper volumes and they should not overlap in the coordinate

space. In the Van der Waals excluded volume approximation this is achieved by replacing the total volume  $V$  in Eq. (3) by the free (available) volume  $V_f \equiv V - b \sum_k k n_k$ , where  $b = 1/\rho_o$  ( $\rho_o = 0.16 \text{ fm}^{-3}$  is the normal nuclear density). Therefore, the corrected CPF becomes:  $Z_A(V, T) = Z_A^{id}(V - bA, T)$ .

The calculation of  $Z_A(V, T)$  is difficult because of the constraint  $\sum_k k n_k = A$ . This difficulty can be partly avoided by calculating the grand canonical partition function:

$$\mathcal{Z}(V, T, \mu) \equiv \sum_{A=0}^{\infty} \exp(\mu A/T) Z_A(V, T) \Theta(V - bA), \quad (4)$$

where the chemical potential  $\mu$  is introduced. The calculation of  $\mathcal{Z}$  is still rather difficult. The summation over the sets  $\{n_k\}$  in  $Z_A$  cannot be performed analytically because of the additional  $A$ -dependence in the free volume  $V_f$  and the restriction  $V_f > 0$ . The problem can be solved by introducing the so-called isobaric partition function (IPF) which is calculated in a straightforward way (see details in Refs. [7, 8, 9, 10]):

$$\hat{\mathcal{Z}}(s, T, \mu) \equiv \int_0^{\infty} dV \exp(-sV) \mathcal{Z}(V, T, \mu) = \frac{1}{s - \mathcal{F}(s, T, \mu)}, \quad (5)$$

where

$$\begin{aligned} \mathcal{F}(s, T, \mu) = & \left(\frac{mT}{2\pi}\right)^{3/2} \left[ z_1 \exp\left(\frac{\mu - sbT}{T}\right) \right. \\ & \left. + \sum_{k=2}^{\infty} k^{3/2-\tau} \exp\left(\frac{(\nu - sbT)k - \sigma k^{2/3}}{T}\right) \right], \end{aligned} \quad (6)$$

with  $\nu \equiv \mu + W_o + T^2/\epsilon_o$ . In the thermodynamic limit  $V \rightarrow \infty$  the pressure of the system is defined by the farthest-right singularity,  $s^*(T, \mu)$ , of the IPF  $\hat{\mathcal{Z}}(s, T, \mu)$

$$p(T, \mu) \equiv T \lim_{V \rightarrow \infty} \frac{\ln \mathcal{Z}(V, T, \mu)}{V} = T s^*(T, \mu). \quad (7)$$

The study of the system's behavior in the thermodynamic limit is therefore reduced to the investigation of the singularities of  $\hat{\mathcal{Z}}$ .

The IPF (5) has two types of singularities: 1) the simple pole singularity defined by the following equation  $s_g(T, \mu) = \mathcal{F}(s_g, T, \mu)$ ; 2) the singularity of the function  $\mathcal{F}$  itself at the point  $s_l(T, \mu) = \nu/Tb$  where the coefficient in linear over  $k$  terms of the exponent in Eq. (6) is equal to zero.

The simple pole singularity corresponds to the gaseous phase where pressure  $p_g \equiv T s_g$  is determined by the following transcendental equation:  $p_g(T, \mu) = T \mathcal{F}(p_g/T, T, \mu)$ . The singularity  $s_l(T, \mu)$  of the function  $\mathcal{F}$  defines the liquid pressure:  $p_l(T, \mu) \equiv T s_l(T, \mu) = \nu/b$ . Here the liquid is represented by an infinite fragment (condensate) with  $k = \infty$ .

In the region of the  $(T, \mu)$ -plane where  $\nu < b p_g(T, \mu)$  the gaseous phase is realized ( $p_g > p_l$ ), while the liquid phase dominates at  $\nu > b p_g(T, \mu)$ . The liquid-gas phase transition occurs when the two singularities coincide, i.e.  $s_g(T, \mu) = s_l(T, \mu)$ . As  $\mathcal{F}$  in Eq. (6) is a monotonously decreasing function of  $s$  the necessary condition for the phase transition is that the function  $\mathcal{F}$  is finite in its singular point  $s_l$ . At  $\tau = 0$  this condition requires  $\sigma(T) > 0$  and, therefore,  $T < T_c$ . Otherwise,  $\mathcal{F}(s_l, T, \mu) = \infty$  and the system is always in the gaseous phase as  $s_g > s_l$ . As one can see from Eq.(6) the convergence

properties of  $\mathcal{F}(s, T, \mu)$  depend significantly on the Fisher's exponent  $\tau$  in the vicinity of the critical point where the surface term vanishes. In what follows we mainly concentrate on the case  $\tau = 0$ . Other possibilities which appear at  $\tau > 0$  are discussed shortly. Their detail study can be found in Ref. [7]. Here we only note that Eqs. (5, 6) represent an exact solution of the Fisher's droplet model [11] where additionally the effects of excluded volume are incorporated.

The baryonic density  $\rho$  in the liquid and gaseous phases is given by the following formulae, respectively:

$$\rho_l \equiv (\partial p_l / \partial \mu)_T = 1/b, \quad \rho_g \equiv (\partial p_g / \partial \mu)_T = \rho_{id} / (1 + b\rho_{id}), \quad (8)$$

where the function  $\rho_{id}$  is the density of point-like nuclear fragments with shifted,  $\mu \rightarrow \mu - bp_g$ , chemical potential:

$$\begin{aligned} \rho_{id}(T, \mu) &= \left(\frac{mT}{2\pi}\right)^{3/2} \left[ z_1 \exp\left(\frac{\mu - bp_g}{T}\right) \right. \\ &\quad \left. + \sum_{k=2}^{\infty} k^{5/2} \exp\left(\frac{(\nu - bp_g)k - \sigma k^{2/3}}{T}\right) \right]. \end{aligned} \quad (9)$$

At  $T < T_c$  the system undergoes a 1-st order phase transition across the line  $\mu^* = \mu^*(T)$  defined by the condition of coinciding singularities:  $s_l = s_g$ , i.e.,  $p_l = p_g$ . The phase transition line  $\mu^*(T)$  in the  $(T, \mu)$ -plane corresponds to the mixed liquid and gas states. This line is transformed into the finite mixed-phase region in the  $(T, \rho)$ -plane shown in Fig. 1. The baryonic density in the mixed phase is a superposition of the liquid and gas baryonic densities:  $\rho = \lambda\rho_l + (1 - \lambda)\rho_g$ , where  $\lambda$  ( $0 < \lambda < 1$ ) is the fraction of the system's volume occupied by the liquid inside the mixed phase. Similar linear combinations are also valid for the entropy density  $s$  and the energy density  $\varepsilon$  with ( $i = l, g$ )  $s_i = (\partial p_i / \partial T)_\mu$ ,  $\varepsilon_i = T(\partial p_i / \partial T)_\mu + \mu(\partial p_i / \partial \mu)_T - p_i$ .

Inside the mixed phase at constant density  $\rho$  the parameter  $\lambda$  has a specific temperature dependence shown in Fig. 2: from an approximately constant value  $\rho/\rho_o$  at small  $T$  the function  $\lambda(T)$  drops to zero in a narrow vicinity of the boundary separating the mixed phase and the pure gaseous phase. This corresponds to a fast change of the configurations from the state which is dominated by one infinite liquid fragment to the gaseous multifragment configurations. It happens inside the mixed phase without discontinuities in the thermodynamical functions.

An abrupt decrease of  $\lambda(T)$  near this boundary causes a strong increase of the energy density as a function of temperature. This is evident from Fig. 3 which shows the caloric curves at different baryonic densities. One can clearly see a leveling of temperature at energies per nucleon between 10 and 20 MeV. As a consequence this leads to a sharp peak in the specific heat per nucleon at constant density,  $c_\rho(T) \equiv (\partial \varepsilon / \partial T)_\rho / \rho$ , presented in Fig. 4. A finite discontinuity of  $c_\rho(T)$  arises at the boundary between the mixed phase and the gaseous phase. This finite discontinuity is caused by the fact that  $\lambda(T) = 0$ , but  $(\partial \lambda / \partial T)_\rho \neq 0$  at this boundary (see Fig. 2).

The negative values of the specific heat shown in Fig. 4 appear due to the parameterization of the surface tension (2): its second derivative with respect to temperature generates a negative contribution in the vicinity of  $T_c$  for all densities. This feature of the model is unphysical and it has to be modified.

It should be emphasized that the energy density is continuous at the boundary of the mixed phase and the gaseous phase, hence the sharpness of the peak in  $c_\rho$  is entirely due to the strong temperature dependence of  $\lambda(T)$  near this boundary. Moreover, at any  $\rho < \rho_o$  the maximum value of  $c_\rho$  remains finite and the peak width in  $c_\rho(T)$  is nonzero in the thermodynamic limit considered in our study. This is in contradiction with the expectation of Refs. [4, 5] that an infinite peak of zero width will appear in  $c_\rho(T)$  in this limit. Also a comment about the so-called “boiling point” is appropriate here. This is a discontinuity in the energy density  $\varepsilon(T)$  or, equivalently, a plateau in the temperature as a function of the excitation energy. Our analysis shows that this type of behavior indeed happens at constant pressure, but not at constant density! This is similar to the usual picture of a liquid-gas phase transition. In Refs. [4, 5] a rapid increase of the energy density as a function of temperature at fixed  $\rho$  near the boundary of the mixed and gaseous phases (see Fig. 3) was misinterpreted as a manifestation of the “boiling point”.

The results presented in Figs. 1-4 are obtained for  $\tau = 0$ . New possibilities appear at non-zero values of the parameter  $\tau$ . At  $0 < \tau \leq 5/2$  the qualitative picture remains the same as discussed above, although there are some quantitative changes. For  $\tau > 5/2$  the condition  $\mathcal{F}(s, T, \mu) < \infty$  is also satisfied in the singularity point  $s_l(T, \mu)$  for all  $T > T_c$  where  $\sigma(T) = 0$ . Therefore, the liquid-gas phase transition extends now to all temperatures. Its properties are, however, different for  $\tau > 7/2$  and for  $\tau < 7/2$  (see Fig. 5). If  $\tau > 7/2$  the gas density is always lower than  $1/b$  as  $\rho_{id}$  is finite. Therefore, the liquid-gas transition at  $T > T_c$  remains the 1-st order phase transition with discontinuities of baryonic density, entropy and energy densities.

At  $5/2 < \tau < 7/2$  the baryonic density of the gas in the mixed phase,  $\rho_g^{mix} \equiv \rho_{id}^{mix}(T)/(1 + b \rho_{id}^{mix}(T))$ , becomes equal to that of the liquid at  $T > T_c$ , i.e.,  $\rho_g^{mix} = 1/b \equiv \rho_o$ , since

$$\begin{aligned} \rho_{id}^{mix}(T) \equiv \rho_{id}(T, \mu^*(T)) &= \left(\frac{mT}{2\pi}\right)^{3/2} \left[ z_1 \exp\left(-\frac{W}{T}\right) \right. \\ &\quad \left. + \sum_{k=2}^{\infty} k^{\frac{5}{2}-\tau} \exp\left(-\frac{\sigma k^{2/3}}{T}\right) \right] \rightarrow \infty, \end{aligned} \quad (10)$$

if surface tension vanishes  $\sigma = 0$ . It is easy to prove that the entropy and energy densities for the liquid and gas phases are also equal to each other. There are discontinuities only in the derivatives of these densities over  $T$  and  $\mu$ , i.e.,  $p(T, \mu)$  has discontinuities of its second derivatives. Therefore, the liquid-gas transition at  $T > T_c$  for  $5/2 < \tau < 7/2$  becomes the 2-nd order phase transition. According to standard definition, the point  $T = T_c$ ,  $\rho = 1/b$  separating the first and second order transitions is the tricritical point. One can see that this point is now at a finite pressure.

It is interesting to note that at  $\tau > 0$  the mixed phase boundary shown in Fig.5 is not so steep function of  $T$  as in the case  $\tau = 0$  presented in Fig.1. Therefore, the peak in the specific heat discussed above becomes less pronounced.

In conclusion, the simplified version of the SMM is solved analytically in the grand canonical ensemble. The progress is achieved by reducing the description of phase transitions to the investigation of the isobaric partition function singularities. The model clearly demonstrates a 1-st order phase transition of the liquid-gas type. The considered system has peculiar properties near the boundary of the mixed and gaseous phases. The rapid change of the thermodynamical functions with  $T$  at fixed  $\rho$  takes place near this

boundary due to the disappearance of the infinite liquid fragment. This leads to leveling of the caloric curves shown in Fig. 3 at temperatures between 6 – 10 MeV depending on the density. As a consequence a sharp peak and a finite discontinuity are developed in the specific heat  $c_p(T)$  at the boundary of the mixed and gaseous phases.

The phase diagram appears to be rather sensitive to the value of the parameter  $\tau$  in the Fisher's free energy term included in our treatment. New interesting possibilities for the phase diagram emerge for  $\tau > 5/2$  in comparison with the case when  $\tau < 5/2$ . The case  $5/2 < \tau < 7/2$  is particularly interesting because of the appearance of the tricritical point separating the 1-st and 2-nd order phase transitions.

### Acknowledgments.

The authors are grateful to D. Blaschke, J. Polonyi and P.T. Reuter for stimulating discussions. We thank the Alexander von Humboldt Foundation and DAAD (Germany) for the financial support. The research described in this publication was made possible in part by Award No. UP1-2119 of the U.S. Civilian Research & Development Foundation for the Independent States of the Former Soviet Union (CRDF). K.A.B. gratefully acknowledges the warm hospitality of the Particle- and Astrophysics Group of the University of Rostock, where this talk was given.

### References

- [1] J.P. Bondorf, A.S. Botvina, A.S. Iljinov, I.N. Mishustin, K.S. Sneppen, Phys. Rep. **257** (1995) 131.
- [2] D.H.E. Gross, Phys. Rep. **279** (1997) 119.
- [3] K.C. Chase and A.Z. Mekjian, Phys. Rev. **C 52** (1995) R2339.
- [4] S. Das Gupta and A.Z. Mekjian, Phys. Rev. **C 57** (1998) 1361.
- [5] S. Das Gupta, A. Majumder, S. Pratt and A. Mekjian, nucl-th/9903007 (1999).
- [6] S. Das Gupta, A.Z. Mekjian and M.B. Tsang, nucl-th/0009033 (2000).
- [7] K.A. Bugaev, M.I. Gorenstein, I.N. Mishustin and W. Greiner, Phys. Rev. **C62** (2000) 044320.
- [8] M.I. Gorenstein, V.K. Petrov and G.M. Zinovjev, Phys. Lett. **B 106** (1981) 327; M.I. Gorenstein, W. Greiner and S.N. Yang, J. Phys. **G 24** (1998) 725.
- [9] K.A. Bugaev, M.I. Gorenstein, I.N. Mishustin and W. Greiner, **nucl-th/0007062** (2000) 3 p.
- [10] K.A. Bugaev, M.I. Gorenstein, I.N. Mishustin and W. Greiner, **nucl-th/0011055** (2000) 7 p.
- [11] M.E. Fisher, Physics **3** (1967) 255.

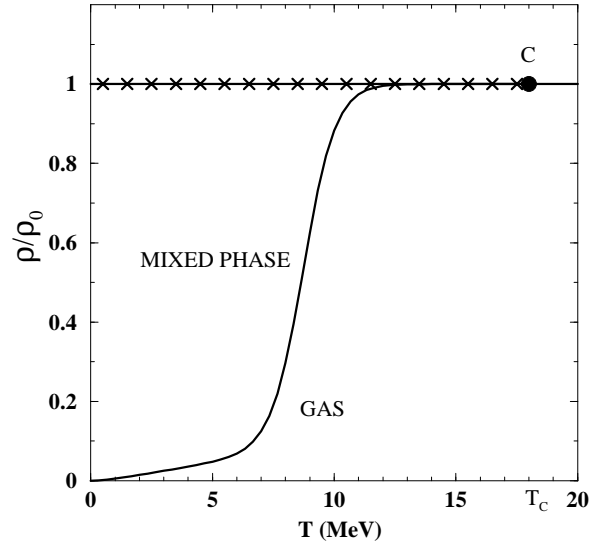


Figure 1: Phase diagram in the  $(T, \rho)$ -plane. The mixed phase and pure gaseous phase boundary is shown by the solid line. The pure liquid phase (shown by crosses) corresponds to the fixed density  $\rho = \rho_0$ . Point  $C$  is the critical point, at  $T > T_c$  only the pure gaseous phase exists.

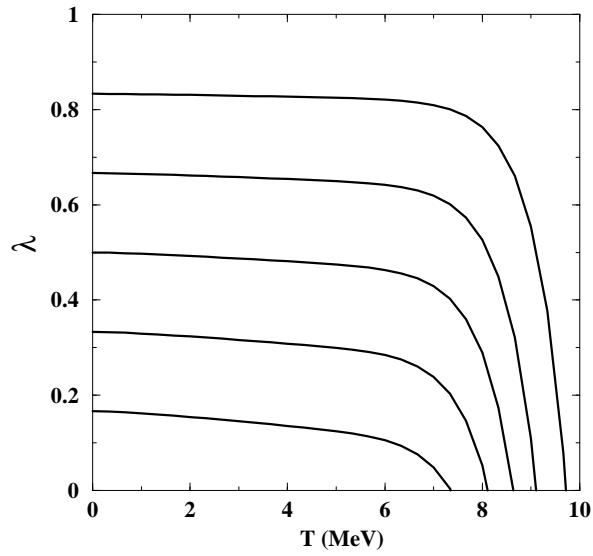


Figure 2: Volume fraction  $\lambda(T)$  of the liquid inside the mixed phase is shown as a function of temperature for fixed nucleon densities  $\rho/\rho_0 = 1/6, 1/3, 1/2, 2/3, 5/6$  (from bottom to top).

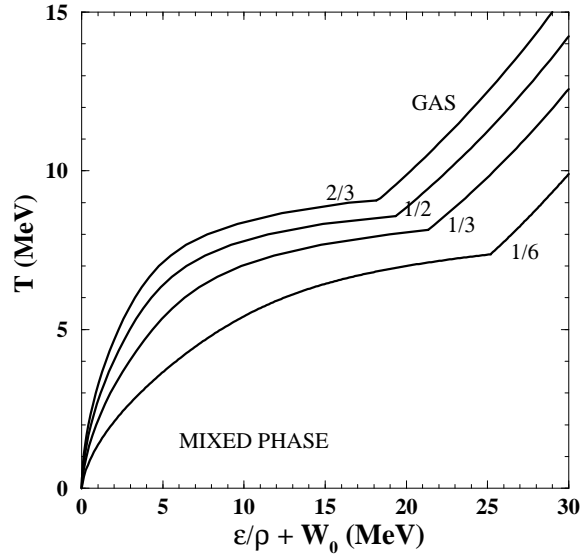


Figure 3: Temperature as a function of energy density per nucleon (caloric curve) is shown for fixed nucleon densities  $\rho/\rho_0 = 1/6, 1/3, 1/2, 2/3$ .

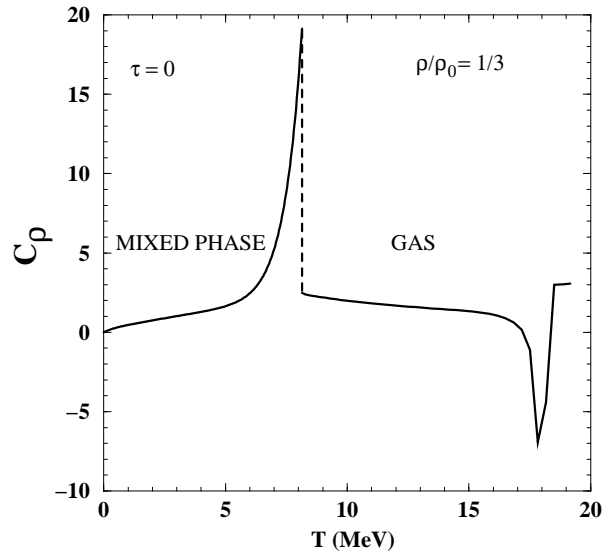


Figure 4: Specific heat per nucleon as a function of temperature at fixed nucleon density  $\rho/\rho_0 = 1/3$ . The dashed line shows the finite discontinuity of  $c_p(T)$  at the boundary of the mixed and gaseous phases. The negative specific heat appears in the vicinity of  $T = 18$  MeV.

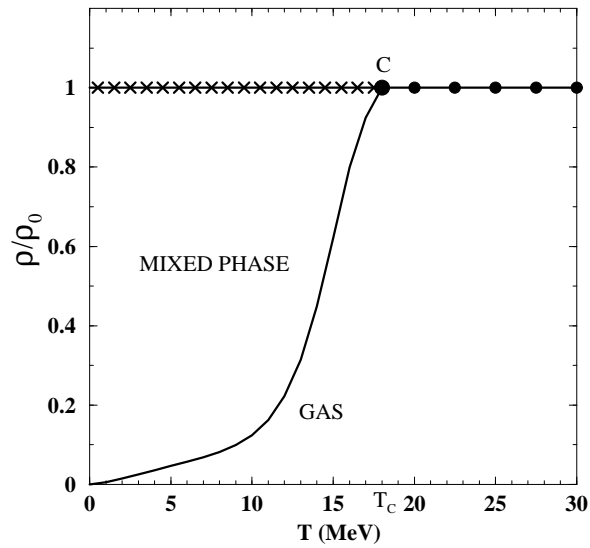
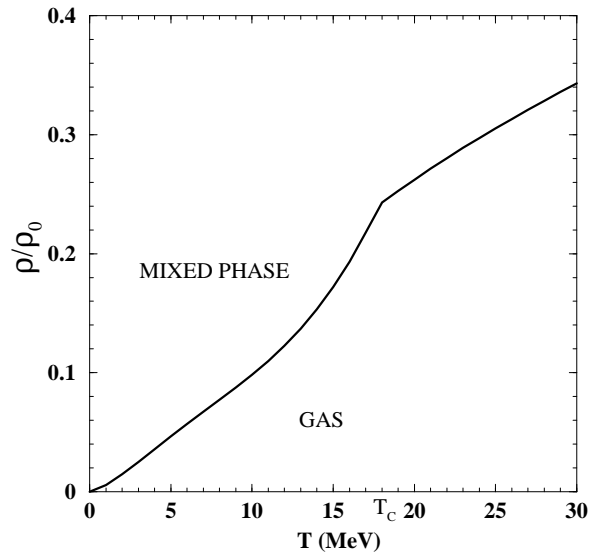


Figure 5: Phase diagrams in  $T - \rho$  plane for  $\tau = 3.6$  (upper panel) and  $\tau = 2.6$  (lower panel). Point  $C$  in the lower panel is the tricritical point. Crosses correspond to the liquid phase of the first order phase transition and dots correspond to the states of the second order one.